Pulse Switching Shock Suppression Method of PWM Inverter for Pole-Changing Induction Motor

H. Kato[1], H. Watanabe[1], J. Itoh[1], and M. Kobayashi[2]
[1] Nagaoka University of Technology, Japan
[2] Toyota Motor Corporation, Japan

***Abstract*-- This paper proposes a pulse switching shock suppression method for a PWM inverter, which consists of two original approaches: (i) a switching method between a synchronous and an asynchronous carrier-based PWM during pole-changing and (ii) a pulse pattern switching method of the synchronous PWM, for a pole-changing induction motor. Continuous changes in harmonic components are confirmed by the proposed method, which suppresses the switching shocks in the analysis and experiment.**

***Index Terms*--Pulse switching shock suppression method, PWM inverter, Induction motor, synchronous PWM**

I. Introduction

In recent years, high-efficiency motors with a wide operating range have been required as drive motors for electric vehicles (EVs) [1][2]. The EV is used in both low-speed-high-torque regions (e.g., starting and hill climbing) and high-speed-low-torque regions (e.g., high-speed cruising). The motor should always be highly efficient in these areas to reduce the size of the cooling system. When a motor of the same volume is considered, a high-pole motor is applied for low-speed, high-torque regions to reduce the impact of the copper loss, which is the dominant factor of the total loss. This motor reduces the phase current due to being less susceptible to magnetic saturation of the back yoke. On the other hand, a low-pole motor, which driven by low frequency compared with the high-pole motor, is applied for high-speed-low-torque regions where the iron loss is the dominant factor of the total loss. Due to increased iron loss depending on the applied frequency, the low-pole motor is expected to be more efficient than the high-pole motor at high speeds. These are a trade-off relationship in motor design. Thus, a switching method for the induction motor (IM) to switch the number of poles according to the operating area has been proposed (Pole-changing IM) [3]. The pole-changing IM switches electrical poles while maintaining a constant rotation speed during operation. In other words, each pole has a different fundamental frequency. The motor efficiency is expected to be improved by driving the motor as a high-pole motor in low-speed, high-torque regions and as a low-pole motor in high-speed, low-torque regions [4].

Inverters installed in EV drive motors use a synchronous PWM to reduce switching loss and noise [5]. The synchronous PWM produces a waveform of the inverter line voltage at every 90 degrees of the electric angles, which reduces the harmonics current of the motor without increasing the switching frequency. The synchronous PWM assumes that the modulated wave is sinusoidal due to its symmetry. However, as mentioned above, the voltage command during pole-changing includes different fundamental frequencies of the two pole numbers. Synchronous PWM cannot be applied due to the asymmetry of this voltage command. As a result, a voltage error, which causes acoustic noise and vibration, occurs when switching from synchronous PWM to asynchronous carrier-based PWM during pole-changing.

On the other hand, the synchronous PWM is used except during pole-changing. The following methods have been proposed for deriving synchronous PWM: a method using carriers with frequencies $3+6n$ times (n: zero and natural numbers) the frequency of the fundamental waveform, and a minimization method of the current RMS value or iron loss [6]-[8]. In these methods, the switching angles shift steeply when the number of pulses or voltage command value changes because the transition pattern of spatial vectors is not taken into account. This generates noise and vibration.

This paper proposes a modulation method of inverters specialized for pole-changing IM to solve the changing pulse pattern problems. The proposed method consists of two original approaches: (i) a switching method between a synchronous and an asynchronous carrier-based PWM during the pole-changing, and (ii) a pulse pattern switching method of the synchronous PWM. The frequency characteristics are maintained before and after by injecting the harmonic components into the voltage command of asynchronous carrier-based PWM in (i). The pulse patterns are proposed in which the switching angles vary continuously even when the voltage or the number of pulses is changed by fixing the transition pattern of the space vector, focusing on the switching sequence of three phase in (ii). The validity of the proposed method is demonstrated by the experiment.

II. Proposed Switching Shock Reduction Method

The proposed method consists of two approaches. First, the modulation method for pole number switching is explained, followed by the method for determining the pulse pattern.

A. Modulation Method During Pole-Changing

Fig. 1 shows the phase voltage command during the pole-changing. In the pole-changing IM, the synchronous PWM cannot be used because the voltage command during pole-changing is an asymmetrical waveform. Thus, switching from the synchronous PWM to the asynchronous carrier-based PWM is necessary when the number of poles is changed. However, switching between the synchronous PWM and the asynchronous PWM with and without low-order harmonics causes a shock due to the steep change in harmonic components.

Fig. 2 shows the harmonic components of the phase voltage included in the synchronous PWM. Fig. 2(b) is derived by subtracting the fundamental component from the synchronous PWM waveform in Fig. 2(a). To keep the harmonic components unchanged when switching between the synchronous PWM and the asynchronous carrier-based PWM, the voltage command in the asynchronous carrier-based PWM should include the harmonic components shown in Fig. 2(b). The phase voltage command V_{ref} in the asynchronous carrier-based PWM is shown in

$$V_{\mathrm{ref}} = V_{\mathrm{fnd.}}(t) + w_1 \cdot V_{\mathrm{hrm.}}(t) \qquad (1)$$

where $V_{\mathrm{fnd.}}(t)$ is the fundamental component of the phase voltage command, $V_{\mathrm{hrm.}}(t)$ is the harmonic components included by the synchronous PWM, and w_1 is the weighting coefficient. V_{ref} is modulated with w_1=1 when switching from the synchronous PWM to the asynchronous carrier-based PWM. Then, the harmonic components can be continuously reduced by changing w_1 from 1 to 0. After switching the number of poles, the same procedure is used to switch to synchronous PWM.

B. Pulse Pattern Switching Method

First, the determining method of the switching phase when the voltage command changes is explained. Then, the reduction of the switching shock method when the number of pulse changes is explained.

Fig. 3 shows the partitioned regions of the basic vector and space vector coordinates of the three-phase inverter, and Table 1 shows the transition patterns of the space vectors in the 7-pulse PWM. In the synchronous PWM, the basic unit of the transition pattern of the space vectors is 0–π/9 rad due to the symmetry of the waveform. In the case of the N-pulse PWM, the number of switching m at 0–π/9 rad is (N+1)/2. The switching is determined under the following conditions,

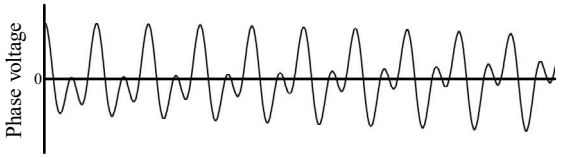

Fig. 1. Phase voltage command during pole-changing.

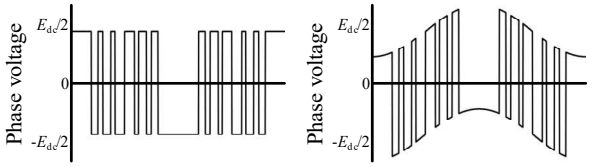

(a) Syn. PWM (b) Harmonic components

Fig. 2. Phase voltage command during pole-changing.

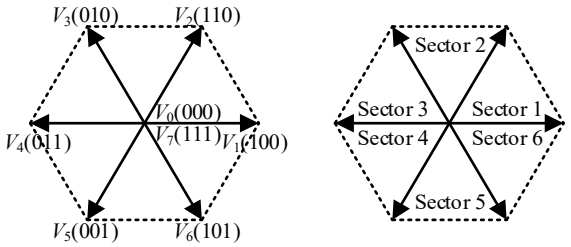

(a) Space vector of three phase inverter (b) Dividing region of space vector

Fig. 3. Transition modes of space vector.

Table 1. Transition mode and switching phase at 0 to 30 deg.

	Transition mode	Switching phase
Mode 1	$V_0 \rightarrow V_1 \rightarrow V_0 \rightarrow V_1$	U→U→U
Mode 2	$V_0 \rightarrow V_1 \rightarrow V_2 \rightarrow V_1$	U→V→V
Mode 3	$V_1 \rightarrow V_0 \rightarrow V_1 \rightarrow V_2$	U→U→V
Mode 4	$V_1 \rightarrow V_2 \rightarrow V_1 \rightarrow V_2$	V→V→V
Mode 5	$V_1 \rightarrow V_2 \rightarrow V_7 \rightarrow V_2$	V→W→W
Mode 6	$V_7 \rightarrow V_2 \rightarrow V_1 \rightarrow V_2$	W→V→V
Mode 7	$V_7 \rightarrow V_2 \rightarrow V_7 \rightarrow V_2$	W→W→W

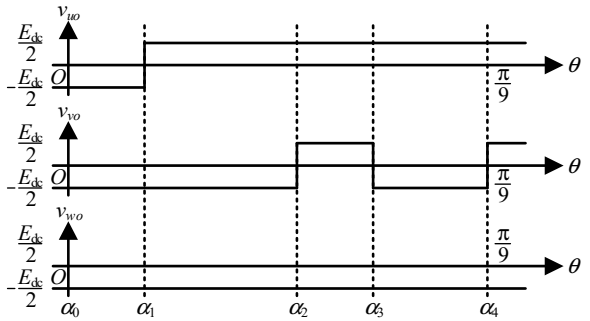

Fig. 4. Phase voltage waveforms at Mode2.

Table 2. Combination of space vector pattern.

	5-pulse PWM	7-pulse PWM	Vector transition
Case 1	$V_0 \rightarrow V_1 \rightarrow V_0$	$V_0 \rightarrow V_1 \rightarrow V_0 \rightarrow V_1$	Continuous
Case 2	$V_0 \rightarrow V_1 \rightarrow V_0$	$V_1 \rightarrow V_0 \rightarrow V_1 \rightarrow V_0$	Continuous
Case 3	$V_0 \rightarrow V_1 \rightarrow V_0$	$V_0 \rightarrow V_1 \rightarrow V_2 \rightarrow V_1$	Discontinuous
Case 4	$V_0 \rightarrow V_1 \rightarrow V_0$	$V_1 \rightarrow V_2 \rightarrow V_7 \rightarrow V_2$	Discontinuous
Case 5	$V_7 \rightarrow V_2 \rightarrow V_1$	$V_7 \rightarrow V_2 \rightarrow V_1 \rightarrow V_2$	Continuous
Case 6	$V_7 \rightarrow V_2 \rightarrow V_1$	$V_0 \rightarrow V_1 \rightarrow V_0 \rightarrow V_1$	Discontinuous
Case 7	$V_7 \rightarrow V_2 \rightarrow V_1$	$V_1 \rightarrow V_2 \rightarrow V_7 \rightarrow V_2$	Discontinuous

- One switch per vector transition.
- No switching at 0 rad.
- Vector at 0 rad can be output in both Sectors 1 and 6.
- Switching at π/9 rad.
- Vectors before and after π/9 rad are nonzero.

From the above, there are transition patterns of the vectors shown in Table 1 with the 7-pulse PWM.

Fig. 4 shows the switching patterns in the case of "Mode 2" of Table 1. In this method, the transition pattern of the space vectors is fixed by defining the phase to be switched from α_1 to α_m in advance when deriving the pulse pattern. The equation for converting U, V, and W-phase switching α_i to U-phase switching β_j is expressed as (2),

$$\begin{cases} \beta_j = \alpha_i & (\text{U-phase switching}) \\ \beta_j = \pi/3 + \alpha_i & (\text{V-phase switching}) \\ \beta_j = \pi/3 - \alpha_i & (\text{W-phase switching}) \end{cases} \quad (2)$$

The fundamental wave amplitude a_1 of the U-phase voltage v_{uo} is expressed by

$$a_1 = \frac{4}{\pi}\int_0^{\pi/2} v_{uo}\cos\theta \mathrm{d}\theta \quad (3)$$

Expanding with β_j yields (4),

$$a_1 = sign\{v_{uo}(0)\}\frac{2E_{\mathrm{dc}}}{\pi}\left\{2\sum_{i=1}^{m-1}(-1)^{i+1}\sin\beta_i - (-1)^m\right\} \quad (4)$$

For simplicity, (5) is obtained by standardizing the square wave voltage by its maximum amplitude $2E_{\mathrm{dc}}/\pi$.

$$\begin{aligned} K_e &= \frac{a_1}{2E_{dc}/\pi} \\ &= sign\{v_{uo}(0)\}\cdot\left\{2\sum_{i=1}^{m-1}(-1)^{i+1}\sin\beta_i - (-1)^m\right\} \end{aligned} \quad (5)$$

K_e is a constraint on the phase voltage command. After that, the pulse pattern is optimized by using the current RMS value of the U-V line currents as an evaluation function, as in the method described in Ref. [6]. The method in Ref. [6] optimizes the switching angles of the U-phase at 0–π/4 rad. On the other hand, the proposed method optimizes the switching angles of the U, V, and W-phase at 0–π/9 rad, which fixes the transition pattern of the space vectors.

The reducing the switching shock method when the number of pulses is changed is described. This method focuses on the transition pattern of space vectors before and after the number of pulses is changed.

Table 2 shows the transition pattern of the space vectors before and after switching between 5 and 7-pulse synchronous PWM. The change in the transition pattern of the space vectors before and after switching must be minimized to reduce the gaps in the switching angles. In the 5 and 7-pulse, an additional vector must be selected that is adjacent to the first or last vector of the 5-pulse. The pulse pattern that is "Continuous" in "Vector transition" in Table 2 is selected. Note that the pulse pattern is optimized based on the transition pattern of the space vectors determined above. Finally, the switching angles while switching the number of pulses is determined by (6) using the weight coefficients w_2,

$$\begin{aligned} \alpha_i = w_2\alpha_{i\_\text{N-pulse}} + (1-w_2)\alpha_{i\_\text{N-1-pulse}}, \\ i: 1,2,3,\cdots(N+1)/2 \end{aligned} \quad (6)$$

The number of pulses is N-1 when w_2=0 and N when w_2=1 in (9). The harmonic components can be changed continuously by changing w_2 from 1 to 0.

III. Simulation Result

Fig. 5 shows the simulation results and harmonic analysis results when switching between the synchronous PWM and the asynchronous carrier-based PWM for pole-changing. The proposed method suppresses the steep change of harmonics immediately after switching that occurs in the conventional method. Besides, the proposed method maintains the same fundamental component during pole-changing.

Fig. 6 shows the pulse pattern optimization results and the current RMS values when the voltage command changes. In the conventional method, the switching angles obtained by optimization have gaps because there are local solutions of the switching angles for each transition pattern of the space vectors. The switching angles do not have gaps by fixing the transition pattern of space vectors in the proposed method. In addition, the increase of the current RMS values due to the application of the proposed method is suppressed to 0.09% at maximum.

Fig. 7 shows the simulation results and harmonic analysis results when the number of pulses changes. When the number of pulses is changed, the proposed method suppresses the steep change of harmonic components that occurs in the conventional method. The fundamental amplitude is kept constant when the number of pulses is changed by changing the switching angles linearly with the weighting coefficient.

IV. Experimental Result

Fig. 8 shows the experimental results and harmonic analysis results when switching between the synchronous PWM and the asynchronous carrier-based PWM for pole-changing. Pole-changing IM with a rated speed of 1800rpm and a rated torque of 11.67Nm. The motor operates 4-pole and 8-pole. The number of poles is changed at no-load, rated speed. The proposed method suppresses the steep change of harmonics immediately after switching that occurs in the conventional method, similar to the simulation results. Low-order harmonic components do not occur during pole switching because the carrier frequency of the asynchronous carrier-based PWM is set to 20kHz, which is far enough away from the fundamental frequency.

Fig. 9 shows the experimental results and harmonic analysis results when the number of pulses changes. The proposed method, suppresses the steep change of harmonics immediately after switching that occurs in the conventional method similar to the simulation results.

V. Conclusions

This paper proposed a new modulation method to suppress a switching shock in a pole-changing induction motor. The switching shock was suppressed by injecting the harmonic components that synchronous PWM includes into the voltage command of asynchronous carrier-based PWM before and after pole-changing in (i). In addition, the switching shock, when the pulse pattern changes, was suppressed with the maximum increase in current RMS value of 0.09% by limiting the transition pattern of the space vectors in the synchronous PWM in (ii). Both methods achieved zero shift in switching angles caused by switching the pulse patterns. The suppression of the switching shock with the proposed method was demonstrated in the analysis and experiment.

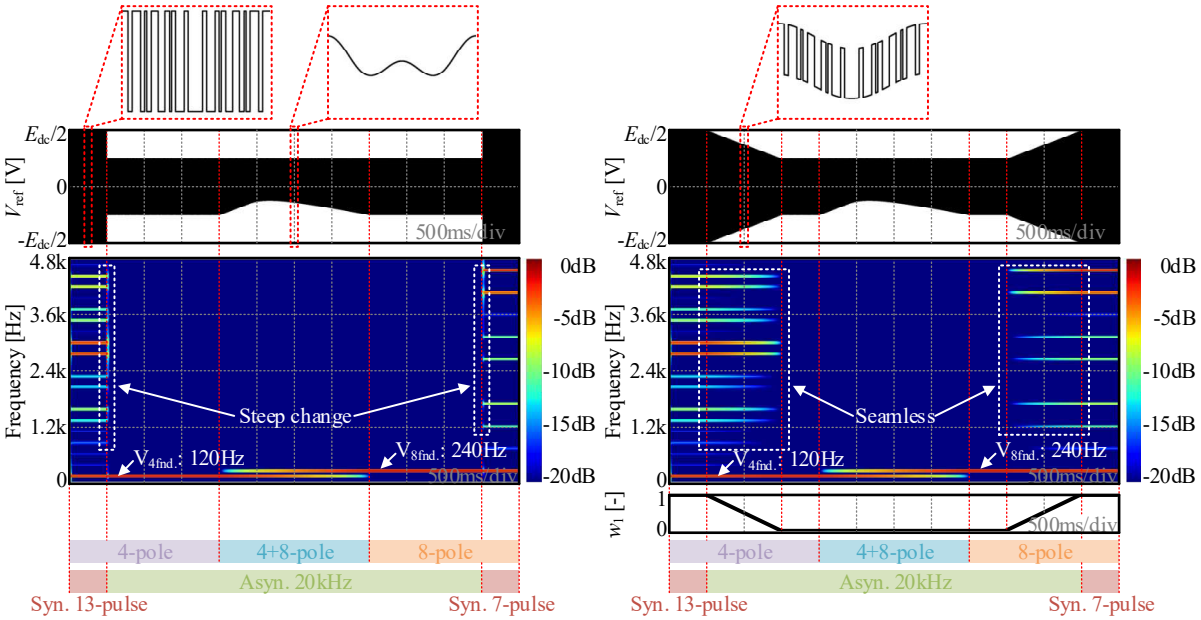

Fig. 5. Simulation results and harmonic analysis results when switching between the synchronous PWM and the asynchronous carrier-based PWM for pole-changing.

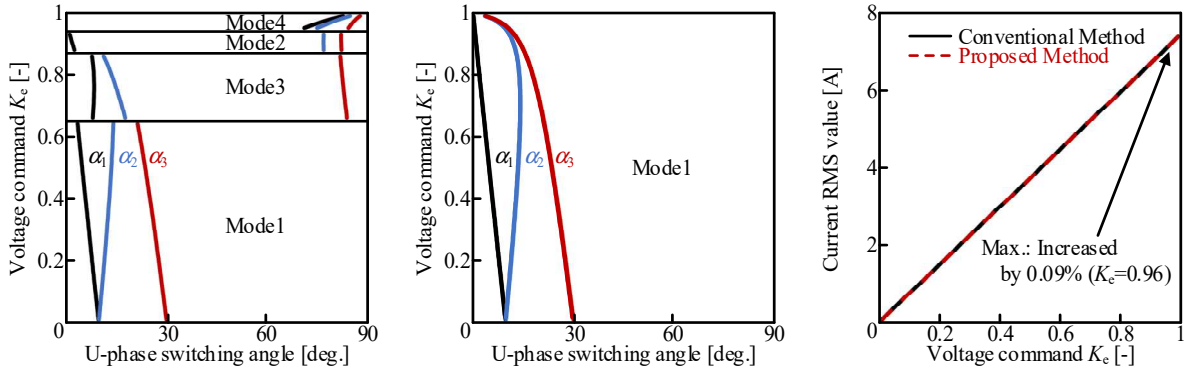

(a) Conventional method (b) Proposed method (c) Current RMS value

Fig. 6. Pulse pattern optimization results and the current RMS values when the voltage command changes.

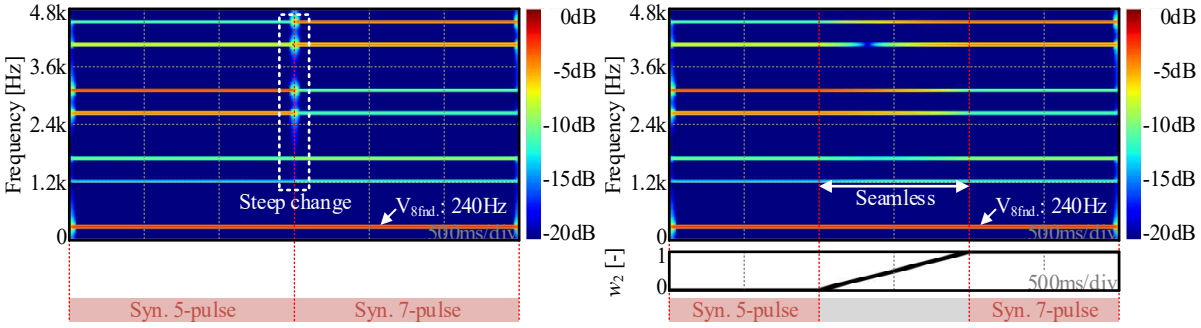

Fig. 7. Simulation results and harmonic analysis results when the number of pulses changes.

REFERENCES

[1] T. Kato, M. Minowa, H. Hijikata, K. Akatsu and R. D. Lorenz, "Design Methodology for Variable Leakage Flux IPM for Automobile Traction Drives," IEEE Transactions on Industry Applications, Vol. 51, No. 5, pp. 3811-3821 (2015)

[2] N. Denis, M. R. Dubois, J. P. F. Trovão and A. Desrochers, "Power Split Strategy Optimization of a Plug-in Parallel Hybrid Electric Vehicle," IEEE Transactions on Vehicular Technology, Vol. 67, No. 1, pp. 315-326 (2018)

[3] Mori M, Mizuno T, Ashikaga T, Matsuda I, "A control method of an inverter-fed six-phase pole change induction motor for electric vehicles," IEEJ Transactions on Industry Applications, Vol. 117, No. 6, pp. 688-695 (1997)

[4] Y. Hidaka, F. Takagi, T. Komatsu, H. Arita, "A novel pole-changing method with multiple three-phase inverters," IEEJ Transactions on Electrical and Electronic Engineering, Vol. 12, No. 12, pp. 1842-1850 (2019)

[5] H. Matsumori, T. Kosaka, N. Matsui and S. Saha, "Alternative PWM Switching Strategy Implementation for a Dual Inverter Fed Open Winding Motor Drive System for an Electric Vehicle Application," IEEE Transactions on Industry Applications, Vol. 59, No. 5, pp. 5957-5970 (2023)

[6] I. Takahashi and H. Mochikawa, "A New Control of PWM Inverter Waveform for Minimum Loss Operation of an Induction Motor Drive," IEEE Transactions on Industry Applications, vol. IA-21, no. 3, pp. 580-587 (1985)

[7] M. A. W. Begh, P. Karamanakos and T. Geyer, "Gradient-Based Predictive Pulse Pattern Control of Medium-Voltage Drives—Part I: Control, Concept, and Analysis," IEEE Transactions on Power Electronics, vol. 37, no. 12, pp. 14222-14236 (2022)

[8] T. Kumagai, T. Ito, K. Nishikawa, J. Itoh, K. Yamane, N. Yamada, and M. Nawa, "Reduction of Iron Loss in Stator Core using an Optimum Pulse Pattern for High-Speed IPMSM," IEEJ Transactions on Industry Applications, vol. 141, no. 4, pp. 313-323 (2021)

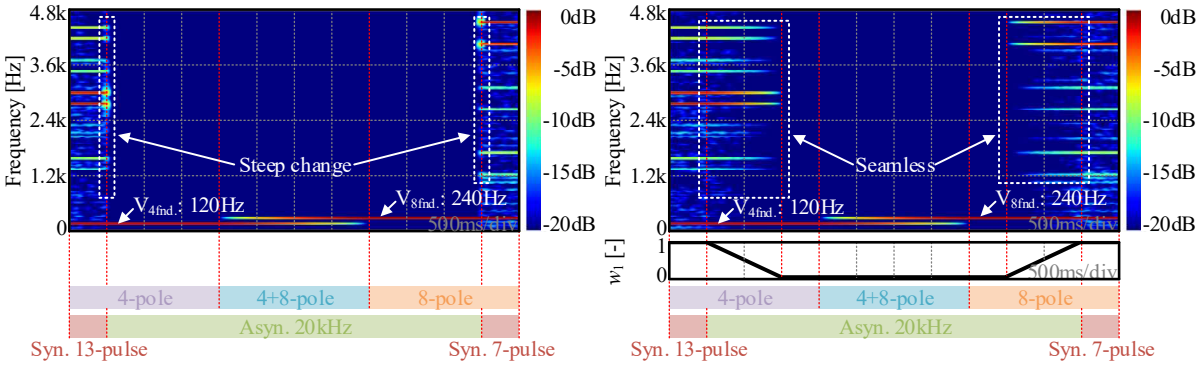

Fig. 8. Experimental results and harmonic analysis results
when switching between the synchronous PWM and the asynchronous carrier-based PWM for pole-changing.

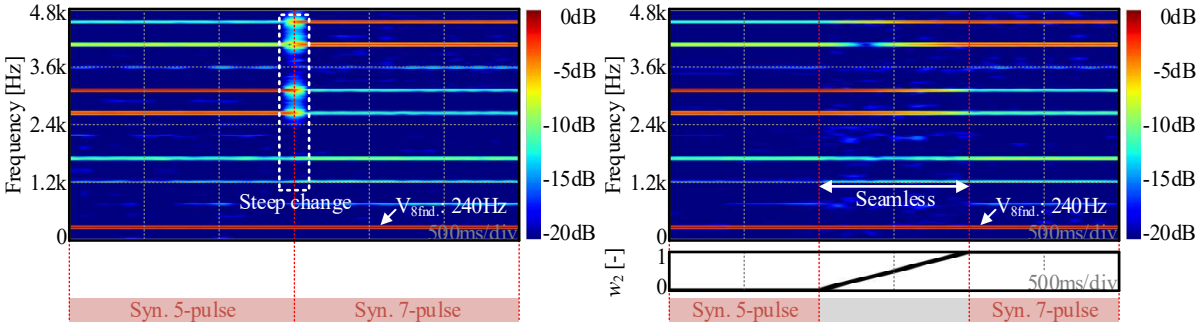

Fig. 9. Experimental results and harmonic analysis results when the number of pulses changes.